Interpretation of the ^{119}Sn Mössbauer isomer shifts in complex tin chalcogenides

P. E. Lippens*
Laboratoire des Agrégats Moléculaires et Matériaux Inorganiques, CNRS ESA 5072, Université Montpellier II, Place Eugène Bataillon, F-34095 Montpellier Cédex 05, France
(Received 25 February 1999)

The main observed trends in the variations of the ^{119}Sn Mössbauer isomer shift δ for tin chalcogenides are interpreted in terms of the valence electronic populations, and are related to changes in the Sn local environment. First, the values of the valence electron charge density at the nucleus $\rho_v(0)$ have been evaluated from a tight-binding calculation for a number of binary compounds in order to check the accuracy of the theoretical approach. A linear correlation between the experimental values of δ and the calculated values of $\rho_v(0)$ is obtained, providing a mean square radius of the nucleus in the Mössbauer transition $\Delta\langle r^2\rangle$ in correct agreement with the previously published values. The same approach is applied to tin chalcogenides with complex structures, and a correct linear correlation between $\rho_v(0)$ and δ is obtained. Different series of chalcogenides have been distinguished considering the Sn oxidation state, the type of chalcogen, and the Sn site symmetry. These series correspond to different ranges of experimental values for δ which have been correlated to the calculated values of $\rho_v(0)$ and the Sn valence electron populations. Finally, a molecular model is proposed which gives simple analytical expressions of the numbers of Sn $5s$ and Sn $5p$ electrons as a function of the Sn site symmetry, the type of chalcogen, and the tin-chalcogen interatomic distance. This model provides a rather simple interpretation of the changes in the values of δ for the different series of chalcogenides.
[S0163-1829(99)04628-7]

I. INTRODUCTION

Mössbauer spectroscopy is a widely used technique for the analysis of the local electronic structure or chemical bonding in solids.[1–3] This technique is based on the recoiless emission and resonant absorption of γ rays by nucleus. The influence of the local electronic structure is due to interactions between the nuclear charge distribution and the extranuclear electric and magnetic fields. The Mössbauer isomer shift δ arises from the electrostatic interaction between nuclear and electron charge distributions due to the finite size of the nucleus. The expression of δ is a function of both the changes in the nuclear radius due to the nuclear transitions, $\Delta\langle r^2\rangle$, and the electron density at the nucleus $\rho(0)$.[2] Variations of the electron density at the nucleus can be related to changes in the local electronic structure which are strongly dependent on the local environment (nearest neighbors). Thus variations of the Mössbauer isomer shift for a series of materials with the same Mössbauer element provide valuable information on changes in the chemical bonding.

Tin chalcogenides SnX_2 and SnX, where $X=$S, Se, and Te have been particularly studied for their electronic properties.[4–6] However, there is also a large number of ternary materials containing a third element generally participating in ionic bonds. In this paper the local electronic structure of Sn atoms is investigated for tin chalcogenides with very different Sn local environments considering the large amount of experimental values for the ^{119}Sn Mössbauer isomer shift. The aim of this paper is to explain the observed main trends in the variations of δ from changes in the calculated Sn electronic populations, and to relate them to the Sn local environments. The present interpretation is based on the evaluation of the numbers of Sn valence electrons and the electron density at the nucleus considering the experimentally determined crystal structures.

The electron density at the Sn nucleus $\rho(0)$ has been previously calculated for tin binary compounds from different theoretical methods.[7–11] The correlation between the experimental values of δ and the calculated values of $\rho(0)$ allows one to evaluate the difference in the mean-square nuclear radius $\Delta\langle r^2\rangle$, which provides a calibration of the Mössbauer experiments. At the present time this is the best way of obtaining the nuclear factor, which cannot be accurately evaluated by nuclear models. The most recent theoretical investigations were based on periodic and molecular calculations of $\rho(0)$. Svane and Antoncik[7] used a linear-muffin-tin-orbital method in the atomic-sphere approximation (ASA) for a calculation of both the electronic structure and $\rho(0)$ for α-Sn, β-Sn, SnO_2, $SnMg_2$, SnSb, and SnTe. Their results give a consistent explanation of the experimental data and $\Delta\langle r^2\rangle = 5.6\times10^{-3}$ fm^2. More recently Svane *et al.*[8] carried out a full potential linear-muffin-tin-orbital calculation which mainly differs from the ASA method by a more refined description of the atomic potentials. Considering a large set of Sn compounds covering a wide range of values for δ, the authors obtained a very good correlation between the experimental values of δ and the calculated values of $\rho(0)$ which gives $\Delta\langle r^2\rangle = 7.2\times10^{-3}$ fm^2. Two recent molecular calculations of $\rho(0)$ based on clusters representing the solids have been proposed. Based on the self-consistent charge $X\alpha$ method, Grodzicki *et al.*[9] obtained $\Delta\langle r^2\rangle = 6.8\times10^{-3}$ fm^2, considering very different tin environments. Terra and Guenzburger[10] used a discrete variational method for SnX_4 halides, with $X=$F, Cl, I, and Br, and they found $\Delta\langle r^2\rangle = 9.2\times10^{-3}$ fm^2. In a more recent paper,[11] these authors considered an improved model of the potential and a series of tin compounds covering a wider range of values for δ. They found a value of $\Delta\langle r^2\rangle = 6.6\times10^{-3}$ fm^2 which is close

to that obtained by Svane *et al.*[8] Based on these recent and reliable calculations, the value of $\Delta\langle r^2\rangle$ is expected to be found between about 6 and 7×10^{-3} fm^2.

The aim of this work is to provide a rather simple interpretation of the observed main trends in the variations of δ for binary and ternary tin chalcogenides based on a semiempirical calculation of $\rho(0)$. An analytical expression of $\rho(0)$ as a function of the numbers of tin valence electrons is first derived from the interpolation to the values of $\rho(0)$ obtained for different electron configurations on a Sn free ion by a relativistic calculation. The numbers of Sn valence electrons are evaluated for tin chalcogenides from a tight-binding method following the Slater-Koster scheme.[12] This method is used here because of the complexity of the crystalline structures, which makes a systematic use of first-principles calculations difficult. In addition, such an approach provides a correct description of the electronic structure of complex chalcogenides.[13–16] The interpretation of the Mössbauer isomer shifts is carried out along three steps. First, the valence electron density at the nucleus is evaluated for a large set of tin binary compounds in order to test the accuracy of the present tight-binding scheme. The values of $\rho(0)$ and $\Delta\langle r^2\rangle$ obtained by the present approach are compared with previously published values. Then $\rho(0)$ is evaluated for tin chalcogenides providing an interpretation of the variations of the experimental values of δ in terms of the changes in the Sn valence electron populations. This allows us to distinguish different series of chalcogenides considering the values of δ. Finally, analytical expressions of the numbers of Sn valence electrons are obtained by a molecular model from the simplification of the periodic tight-binding calculation in the case of highly symmetrical Sn environments. This allows us to interpret the observed main trends in the variations of δ as a function of several parameters describing the Sn local environment: the Sn site symmetry, the type of chalcogen nearest neighbors, and the interatomic distances.

The theoretical method used to evaluate the electron density at the nucleus is described in Sec. II. Section III concerns the tight-binding results obtained for tin binary and ternary chalcogenides. The molecular model is developed in Sec. IV, and the conclusions are summarized in Sec. V.

II. THEORETICAL METHOD

The Mössbauer isomer shift (in mm/s) is related to the electronic density at the nucleus (in a_0^{-3}, where a_0 is the Bohr radius) by the relation[17]

$$\delta=\alpha[\rho_a(0)-\rho_s(0)], \tag{1}$$

where $\rho_a(0)$ and $\rho_s(0)$ are the electron densities at the nucleus of the absorber and source, respectively. The isomer shift calibration constant α is a linear function of the change in the mean-square radius of the nucleus in the Mössbauer transition $\Delta\langle r^2\rangle$:

$$\alpha=\beta\Delta\langle r^2\rangle, \tag{2}$$

where β depends only on the characteristics of the Mössbauer isotope and the transition energy, and is equal to $12.7a_0^3$ mm s^{-1} fm^{-2} for ^{119}Sn.[18] Although $\Delta\langle r^2\rangle$ should be evaluated from nuclear calculations, the most accurate values have been obtained by a comparison between the experimental values of the isomer shift and the calculated values of $\rho(0)$ which are expected to be linearly correlated, as shown by Eqs. (1) and (2). The most recent published values[7–11] for ^{119}Sn are found around 7×10^{-3} fm^2. In this paper the value of $\Delta\langle r^2\rangle$ will be determined considering a large number of tin binary compounds with very different chemical bondings, and compared to the previously published values in order to check the accuracy of the present theoretical approach.

The electron density at the ^{119}Sn nucleus $\rho(0)$ arises from contributions of the core electrons $\rho_c(0)$ and the valence electrons $\rho_v(0)$. In this work, the core electron density at the nucleus is assumed to be constant for the different materials (the frozen-core approximation). The validity of this approximation for an analysis of the variations of the Sn Mössbauer isomer shift has been previously discussed.[7] It was shown that for most of the tin chalcogenides, variations of $\rho_c(0)$ are negligible compared to those of $\rho_v(0)$. The valence electron density at the nucleus has been evaluated in two steps. First, an analytical expression of $\rho_v(0)$ as a function of the numbers of Sn $5s$ (N_s) and Sn $5p$ (N_p) valence electrons has been derived from interpolation to the calculated values for different electron configurations of the Sn free ion. Then the values of $\rho_v(0)$ for solids have been evaluated from this expression and the numbers of tin valence electrons obtained by tight-binding calculations.

Following the approach of Ruby and Shenoy,[19] the electron density $\rho_v(0)$ is assumed to be a nonlinear function of both N_s and N_p, and has been fitted to the values of $\rho_v(0)$ calculated by Ellis[19] for Sn free ions:

$$\rho_v(0)=0.76+53.80N_s-0.94N_p-5.00N_s^2-2.80N_sN_p\,. \tag{3}$$

The numbers of Sn valence electrons have been evaluated from a tight-binding calculation following the Slater-Koster formulation.[12] This approach is mainly justified here by the complexity of the crystal structures, and because it produces correct trends in the electronic structure of complex chalcogenides.[13–16] By the Slater-Koster method, the one-electron Schrödinger equation is solved considering a minimal orbital basis set formed here by the s and p valence orbitals of the atoms in the unit cell. The elements of the tight-binding Hamiltonian matrix are expressed in terms of one- and two-center integrals which are considered to be the intra-atomic and interatomic tight-binding parameters, respectively. The intra-atomic terms are the free-atom energy levels calculated by Herman and Skillman[20] and reported by Harrison.[21] The interatomic terms are evaluated from the Robertson scaling law[13,15] and the Harrison parameters.[22] The number of tin valence electrons of type i ($i=s,p$) is defined by

$$N_i=2\sum_{n,\mathbf{k}}|\langle\varphi_i|\psi_{n,\mathbf{k}}\rangle|^2, \tag{4}$$

where φ_i is the atomic orbital, and $\Psi_{n,\mathbf{k}}$ the Bloch wave function for the band n and the wave vector $\mathbf{k}$. The sum runs over the valence bands for n and a grid of points in the first Brillouin zone for $\mathbf{k}$.

TABLE I. Experimental data for the binary tin compounds: structural information; Sn oxidation states; average values of the ^{119}Sn Mössbauer isomer shift δ relative to $BaSnO_3$, with source and absorber at ambient and nitrogen temperatures, respectively, except * absorber at ambient temperature. Calculated values of the numbers of Sn $5s$ electrons, N_s(Sn), and Sn $5p$ electrons, N_p(Sn), and the electron density at the nucleus $\rho_v(0)$. For mixed valency compounds the Sn(IV) and Sn(II) atoms are labeled 1 and 2, respectively.

Compound	Space group	Oxidation state of Sn	δ (mm/s)	N_s(Sn)	N_p(Sn)	$\rho_v(0)$ (a_0^{-3})
SnF_4	$I4/mmm$[a]	IV	-0.4[p]	0.63	1.06	29.8
Sn_2F_6 (1)	$Fm\bar{3}m$[b]	IV	-0.4*[q]	0.71	1.30	32.5
Sn_3F_8 (1)	$P2_1/n$[c]	IV	-0.35*[r]	0.67	1.19	31.2
SnO_2	$P4_2/mnm$[d]	IV	0.0[p]	0.77	1.23	35.5
$SnBr_4$	$P2_1/c$[e]	IV	1.1[p]	1.08	1.30	47.8
Sn_2S_3 (1)	$Pnma$[f]	IV	1.15[s]	1.20	1.41	52.2
SnS_2	$P\bar{3}m_1$[g]	IV	1.3[p]	1.20	1.41	52.0
SnI_4	$Pa3$[h]	IV	1.5[p]	1.31	1.30	56.5
$SnSe_2$	$P\bar{3}m_1$[g]	IV	1.5[p]	1.31	1.51	55.9
$SnMg_2$	$Fm\bar{3}m$[g]	0	1.8[p]	1.69	3.62	56.8
αSn	$Fd3m$[g]	0	2.1[p]	1.66	2.34	63.1
βSn	$I4_1/amd$[g]	0	2.6[p]	1.75	2.25	66.4
SnP	$Fm\bar{3}m$[i]	0	2.7[p]	1.67	1.58	67.7
SnAs	$Fm\bar{3}m$[g]	0	2.7[p]	1.71	1.71	68.5
SnSb	$Fm\bar{3}m$[g]	0	2.8[p]	1.79	1.86	69.9
Sn_4P_3	$R\bar{3}m$[j]	0	2.9[p]	1.86	1.48	74.4
Sn_4As_3	$R\bar{3}m$[j]	0	2.9[p]	1.87	1.56	74.4
SnO	$P4/nmm$[k]	II	2.7[p]	1.88	1.00	78.0
SnSe	$Pnma$[l]	II	3.4[p]	1.95	1.17	79.2
SnS	$Pnma$[l]	II	3.4[p]	1.95	1.07	79.7
SnTe	$Fm\bar{3}m$[g]	II	3.5[p]	1.96	1.30	78.6
Sn_2S_3 (2)	$Pnma$[f]	II	3.5[s]	1.94	1.06	79.5
SnF_2	$C2/c$[m]	II	3.6[p]	1.92	0.71	81.1
Sn_3F_8 (2)	$P2_1/n$[c]	II	3.8*[r]	1.94	0.54	82.8
SnI_2	$C2/m$[n]	II	3.9[p]	1.99	0.90	82.1
$SnCl_2$	$Pnma$[o]	II	4.1[p]	1.98	0.54	84.1
Sn_2F_6 (2)	$Fm\bar{3}m$[b]	II	4.1*[q]	1.96	0.53	83.5

[a]Reference 24.
[b]Reference 25.
[c]Reference 26.
[d]Reference 27.
[e]Reference 28.
[f]Reference 29.
[g]Reference 30.
[h]Reference 31.
[i]Reference 32.
[j]Reference 33.
[k]Reference 34.
[l]Reference 35.
[m]Reference 36.
[n]Reference 37.
[o]Reference 38.
[p]Reference 23.
[q]Refs. 39 and 40.
[r]Average values of Refs. 26 and 40.
[s]Average values of Refs. 41 and 42.

III. RESULTS

A. Tin binary compounds

The aim of this part is to assess the accuracy of the tight-binding calculation of $\rho_v(0)$ for the analysis of the ^{119}Sn Mössbauer isomer shifts considering a series of tin binary compounds. The structural information used in the tight-binding calculations, the tin oxidation states, the experimental values of δ, and the calculated values of N_s, N_p, and $\rho_v(0)$ are reported in Table I. The values of δ relative to $BaSnO_3$ for most of the materials concern measurements with source and absorbing materials at ambient and nitrogen temperatures, respectively. There is now a large amount of experimental values of the ^{119}Sn Mössbauer isomer shift in the literature.[23] However, some differences can be found for a given compound which are probably due to the experimental accuracy or the purity of the materials. Thus average values of δ are reported in Table I for most of the materials which should be correct within about 0.1 mm/s. The values of δ are found between -0.4 and 4.1 mm/s, and cover nearly the whole range of ^{119}Sn Mössbauer isomer shifts. From the chemist's point of view it is of interest to determine the

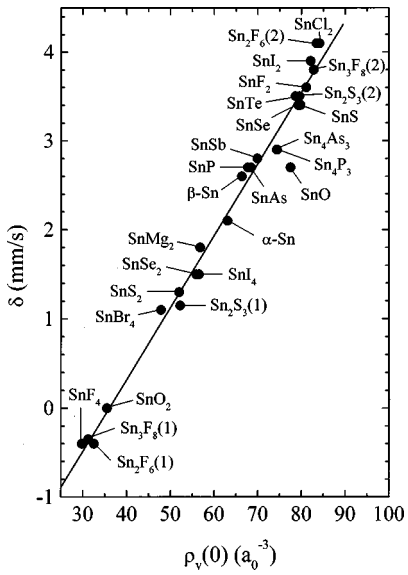

FIG. 1. Experimental values of the ^{119}Sn Mössbauer isomer shift δ against calculated values of the electron density at the nucleus $\rho_v(0)$ for binary tin compounds.

formal oxidation state of tin. This can be easily obtained from Mössbauer measurements, and Table I shows that the values of δ are lower than about 2 mm/s for the Sn(IV) compounds, are found between about 1.8 and 3 mm/s for the Sn(0) compounds, and are greater than about 2.7 mm/s for the Sn(II) compounds. It is worth noticing that Sn_2S_3, Sn_2F_6, and Sn_3F_8 are mixed valency compounds containing both Sn(IV) and Sn(II) oxidation states, as shown experimentally by the existence of two very different values for δ. In principle, the three oxidation states Sn(IV), Sn(0), and Sn(II) should be related to the three sets of values $(N_s, N_p) = (0,0)$, (1,3), and (2,0), respectively. This definition of the formal oxidation state corresponds to a full transfer of electrons. Table I shows that the three tin oxidation states can be correlated to the numbers of Sn $5s$ electrons: 0.6–1.3 for Sn(IV), 1.6–1.8 for Sn(0), and 1.8–2 for Sn(II). The values of N_s for the Sn(IV) and Sn(0) compounds strongly differ from the expected formal values. This may be related to the covalency of the bonds involving the Sn atoms which reduces the electronic transfer from the tin atoms to their nearest neighbors. The numbers of Sn $5p$ electrons in the Sn(IV) compounds are found between 1 and 1.5. These values are close to the number of Sn $5s$ electrons, except for the most ionic compounds such as tin fluorides and SnO_2. For the Sn(II) compounds, the number of Sn $5p$ electrons is lower than the number of Sn $5s$ electrons, which is close to 2. This reflects the electronic transfer of the Sn $5p$ electrons toward the chalcogen nearest neighbors. Finally, similar values of the numbers of Sn $5s$ and Sn $5p$ electrons are found for the Sn(0) compounds except for αSn and $SnMg_2$. For the two latter materials the number of Sn $5p$ electrons is greater than the number of Sn $5s$ electrons due to the sp^3 hybridization of the Sn valence orbitals.

The experimental values of δ are plotted against the calculated values of $\rho_v(0)$ in Fig. 1. A quasilinear correlation is observed, except for SnO, which shows a large departure from the expected value. In the latter case the present tight-binding approach fails in a determination of the electronic populations, and a more refined model is required. The slope of the line obtained by a linear regression to the results gives the value of the nuclear radius change $\langle \Delta r^2 \rangle = 6.4 \times 10^{-3}$ fm^2, which is in correct agreement with the most recent published values found around 7×10^{-3} fm^2. It is difficult to compare the values of the electron density at the nucleus obtained by different calculations because of the observed large differences between the values of the total electron density $\rho(0)$ for a given compound. For example, the orders of magnitude are of about $186\,000 a_0^{-3}$ for the present work, $183\,000 a_0^{-3}$ for the works of Svane and Antoncik[7] and Svane *et al.*,[8] and $190\,000 a_0^{-3}$ for the work of Grodzicki *et al.*[9] However, it is possible to compare the variations of $\rho(0)$ due to changes in the valence electronic populations considering a uniform shift of each set of calculated values. The energy shift was evaluated by a least-mean-square fit of each set of published values to the tight-binding results, and similar trends in the variations of $\rho(0)$ are obtained by the different calculations. The most severe discrepancies occur for some ionic compounds such as SnF_4, SnO_2, and SnO, but a correct agreement is obtained for the tin chalcogenides of present interest. More accurate values of $\rho_v(0)$ for the ionic compounds could in principle be obtained by adjusting the tight-binding parameters. However, such an approach is not expected to improve the results for tin chalcogenides noticeably, justifying the present evaluation of $\rho_v(0)$ from a universal set of tight-binding parameters.

As noticed above, the tin oxidation state can be correlated to the number of Sn $5s$ electrons. These electrons strongly inluence $\rho_v(0)$, which explains the correlation between the Sn Mössbauer isomer shift and the Sn oxidation state. The variations of δ as a function of N_s are shown in Fig. 2, and clearly exhibit a linear trend. The main deviations to this tendency occur for $SnMg_2$, αSn, SnI_2, $SnCl_2$, Sn_3F_8, and Sn_2F_6 (Fig. 2). The calculated values of N_s for $SnMg_2$ and αSn are greater than those expected by the linear correlation, whereas for the four other materials the calculated values of N_s are lower than those expected. This can be explained by the so-called screening effect of the Sn $5p$ electrons upon $\rho_v(0)$, which unlike the Sn $5s$ electrons tend to decrease the electron density at the nucleus. This can be seen from Eq. (3), which shows that $\rho_v(0)$ strongly increases with N_s and slightly decreases with N_p. For most of the compounds considered in this paper, the number of Sn $5p$ electrons is found to be between 1.1 and 1.8. For αSn and $SnMg_2$, N_p is greater than 2.3, and tends to decrease $\rho_v(0)$. For SnI_2, SnF_2, Sn_3F_8, and Sn_2F_6, N_p is lower than 1 and tends to increase $\rho_v(0)$. This explains the improvement in the linearity of δ-$\rho(0)$ (Fig. 1) by comparison with that of δ-N_s (Fig. 2) for these compounds.

In summary, the value of $\langle \Delta r^2 \rangle$ and the variations of $\rho_v(0)$ calculated for a series of tin binary compounds are in correct agreement with previously published results, especially for tin chalcogenides. This shows that the tight-binding method correctly predicts the variations of $\rho_v(0)$ for interpreting the Sn Mössbauer isomer shifts.

B. Tin chalcogenides

This section is devoted to the interpretation of the ^{119}Sn Mössbauer isomer shift for binary and ternary chalcogenides.

In addition to the tin and chalcogen atoms found in binary chalcogenides, the ternary compounds studied in this work also include atoms with only *s* valence electrons (Na, Ba) or with *s* and *p* valence electrons (Ge, In, Sb, Tl, and Pb). The ternary compounds are listed in Table II, with the structural data used in tight-binding calculations, the Sn local environments, the Sn oxidation states, the experimental values of the Mössbauer isomer shift, and the calculated values of N_s, N_p, and $\rho_v(0)$. The values of δ are relative to $BaSnO_3$. Except for $SnBi_2Te_4$, the measurements were performed with source and absorbing materials at ambient and nitrogen temperatures, respectively. Unlike the tin binary compounds there are less data for ternary chalcogenides and the values reported in Table II are not averaged over different published values. Most of the tin ternary compounds have a complex structure due to their low symmetry and the large number of atoms per unit cell. The Sn atoms are always bonded to chalcogen nearest neighbors which form in most cases slightly distorted tetrahedra or octahedra. Informations on binary tin chalcogenides are reported in Table I except for the Sn local structures which are described now. In the Sn(IV) compounds SnS_2 and $SnSe_2$, the tin atoms are octahedrally surrounded by S (2.56 Å) and Se (2.68 Å) atoms, respectively. The tin environments in the Sn(II) binary compounds are trigonal pyramids for SnS (2.65 Å) and SnSe (2.8 Å) considering only the nearest neighbors and very distorded octahedra when including the second-nearest neighbors. SnTe has a rocksalt NaCl structure, and the Sn atoms are octahedrally surrounded by six Te atoms (3.15 Å). In Sn_2S_3 there are two crystallographic sites with different oxidation states Sn(IV) and Sn(II). The Sn(IV) atoms are surrounded by six S atoms forming a slightly distorded octahedron (2.55 Å), and the Sn(II) atoms are bonded to three nearest neighbors (2.7 Å). The values of the Mössbauer isomer shift for both the binary and ternary compounds span the two ranges of values 1–2 and 3.2–3.8 mm/s, which may be related to the two oxidation states Sn(IV) and Sn(II), respectively (Tables I and II). Different series of Sn(IV) compounds can be distinguished from the type of anion and the Sn site symmetry. They correspond to different ranges of values for δ which are found between about 1.1 and 1.4 mm/s for the sulfides, 1.5 and 1.7 mm/s for the selenides, and around 2 mm/s for the tellurides. For the Sn(IV) sulfides with tetrahedral and octahedral tin environments, the values of δ are found within the same range, and it is rather difficult to distinguish these two types of Sn sites from the only values of δ. For the Sn(IV) selenides the difference between the values of δ for the Sn octahedral sites ($\approx$1.5 mm/s) and the Sn tetrahedral sites ($\approx$1.7 mm/s) is more significant. Finally, it seems difficult to establish some main trends in the variations of δ for Sn(II) chalcogenides, and no attempt to interpret the variations of δ within this range of values is made in this paper.

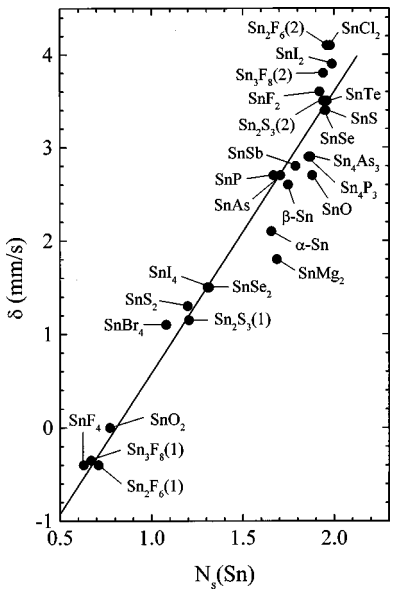

FIG. 2. Experimental values of the ^{119}Sn Mössbauer isomer shift δ against the calculated values of the Sn 5*s* number of electrons N_s(Sn) for binary tin compounds.

The experimental values of δ for both the binary and ternary chalcogenides are plotted against the calculated values of $\rho_v(0)$ in Fig. 3, as well as the straight line obtained in Sec. III A from the correlation between δ and $\rho_v(0)$ for tin binary compounds. Figure 3 shows that the variations of δ as a function of $\rho_v(0)$ are consistent with those of the tin binary compounds. Inspection of Tables I and II shows that the increase of δ from 1–2 mm/s for the Sn(IV) chalcogenides to 3.2–3.8 mm/s for the Sn(II) chalcogenides may be mainly related to the increase in the number of Sn 5*s* electrons from 1.2–1.6 to 1.9–2. The number of Sn 5*p* electrons does not vary noticeably ($\approx$1.3–1.6), except for some Sn(II) compounds, but this has only a minor effect on $\rho_v(0)$. The observed increase of δ for the sequence of Sn(IV) chalcogenides: sulfides ($\delta \approx 1.2$ mm/s)–selenides ($\delta \approx 1.6$ mm/s)–tellurides ($\delta \approx 2$ mm/s) may be correlated to the increase of $\rho_v(0)$ from about $52a_0^{-3}$ to $57a_0^{-3}$, which is mainly due to the increase of N_s from about 1.2 (sulfides) to 1.3 (selenides) and 1.5 (tellurides). Differences between the values of δ for Sn(IV) sulfides with octahedral and tetrahedral Sn local environments are rather small. For the selenides, the increase is more significant: from 1.5 mm/s for $SnSe_2$ to about 1.7 mm/s for Tl_4SnSe_4 and Tl_2SnSe_3, and may be correlated to the increase of both $\rho_v(0)$ and N_s. Finally, the variations of δ are fairly well reproduced by the calculated values of $\rho_v(0)$ for the Sn(II) compounds. Although the observed main trends in the variations of δ may be correlated to those of $\rho_v(0)$, Fig. 3 clearly shows that the present tight-binding approach cannot provide a reliable interpretation of some small variations of δ as observed for some Sn(IV) sulfides or Sn(II) compounds.

In summary, variations of the ^{119}Sn Mössbauer isomer shift for tin chalcogenides are consistent with changes in the calculated electron density at the nucleus which are mainly due to the Sn 5*s* electrons. The main trends in the variations of δ are correlated to the changes in the tin oxidation state and for the Sn(IV) compounds to the type of chalcogen (S, Se, Te) and the Sn site symmetry. The results are summarized in Table III, with the values of δ, N_s, N_p, $\rho_v(0)$ and the tin-chalcogen interatomic distance d all averaged over the different compounds with the same Sn environment.

IV. MOLECULAR MODEL

A. Description of the model

In Sec. III the variations of the Mössbauer isomer shift of tin chalcogenides have been explained from changes in the

TABLE II. Experimental data for ternary tin compounds: space group; Sn site symmetry (the distorted and undistorted forms are not distinguished) [*o*, octahedron; *t*, tetrahedron; *b*, trigonal bipyramid; *d*, trigonal dodecahedron; tp, bicapped trigonal prism; sp, square-based pyramid; and average interatomic distance in parentheses (in Å)]: Sn oxidation state; ^{119}Sn Moössbauer isomer shift δ relative to $BaSnO_3$, with source and absorber at ambient and nitrogen temperatures, respectively, except * absorber at ambient temperature. Calculated values of the numbers of Sn 5*s* electrons, N_s(Sn), and Sn 5*p* electrons, N_p(Sn), and electron density at the nucleus $\rho_v(0)$. For mixed valency compounds the Sn(IV) and Sn(II) atoms are labeled 1 and 2, respectively.

	Compound	Space group	Sn local structure	Oxidation state of Sn	δ (mm/s)	N_s(Sn)	N_p(Sn)	$\rho_v(0)$ (a_0^{-3})
1	$Sn_5Sb_2S_9$ (1)	$Pbca$[a]	*o* (2.58)	IV	1.10[t]	1.21	1.40	52.6
2	$PbSnS_3$	$Pnma$[b]	*o* (2.56)	IV	1.13[u]	1.19	1.43	52.6
3	$Ba_2SnS_4\beta$	$Pna2_1$[c]	*t* (2.37)	IV	1.19[u]	1.17	1.49	50.7
4	$In_2Sn_3S_7$ (1)	$P2_1/m$[d]	*o* (2.62)	IV	1.19[d]	1.24	1.30	53.9
5	$Tl_4Sn_5S_{12}$	$P\bar{1}$[e]	$t+o$ (2.52)	IV	1.22[v]	1.21	1.42	52.3
6	Na_4SnS_4	$P\bar{4}2_1c$[f]	*t* (2.39)	IV	1.23[u]	1.18	1.46	51.1
7	$Na_4Sn_3S_8$	$C2/c$[g]	$t+b$ (2.46)	IV	1.25[u]	1.18	1.44	51.2
8	$Ba_2SnS_4\alpha$	$P2_1/c$[h]	*t* (2.40)	IV	1.27[u]	1.19	1.47	51.3
9	$Tl_2Sn_2S_5$	$C2/c$[i]	*b* (2.50)	IV	1.28[v]	1.22	1.42	52.8
10	$Na_6Sn_2S_7$	$C2/c$[j]	*t* (2.38)	IV	1.28[u]	1.17	1.46	50.8
11	$Ba_3Sn_2S_7$	$P2_1/c$[j]	*t* (2.39)	IV	1.29[u]	1.18	1.47	51.0
12	Tl_4SnS_4	$P2_1/c$[k]	*t* (2.39)	IV	1.35[v]	1.24	1.44	53.5
13	Tl_2SnS_3	$C2/m$[l]	*t* (2.40)	IV	1.41[v]	1.23	1.44	53.1
14	Tl_2SnSe_3	$Pnma$[m]	*t* (2.55)	IV	1.65[w]	1.34	1.49	56.8
15	Tl_4SnSe_4	$P2_1/c$[n]	*t* (2.53)	IV	1.67[w]	1.34	1.52	56.8
16	Tl_2SnTe_5	$I4/mcm$[o]	*t* (2.79)	IV	2.04[x]	1.53	1.63	62.8
17	Tl_2SnTe_3	$Pnma$[p]	*t* (2.78)	IV	2.04[x]	1.55	1.60	63.5
18	$SnBi_2Te_4$	$R\bar{3}m$[q]	*o* (3.14)	II	3.3*[y]	1.96	1.36	78.2
19	$SnSb_2Te_4$	$R\bar{3}m$[q]	*o* (3.09)	II	3.37[z]	1.94	1.43	77.3
20	$Sn_5Sb_2S_9$ (2)	$Pbca$[a]	*d* (3.09)	II	3.39[t]	1.93	1.11	78.8
21	Tl_4SnTe_3	$I4/mcm$[r]	*o* (3.28)	II	3.47[x]	1.97	1.16	80.0
22	$GeSnS_3$	$P2_1/c$[s]	sp (2.86)	II	3.50[aa]	1.95	0.98	80.5
23	$In_2Sn_3S_7$ (2)	$P2_1/m$[d]	tp (3.09)	II	3.82[d]	1.94	0.92	80.4

[a]Reference 43.
[b]Reference 44.
[c]Reference 45.
[d]Reference 42.
[e]Reference 46.
[f]Reference 47.
[g]Reference 48.
[h]Reference 49.
[i]Reference 50.
[j]Reference 51.
[k]Reference 52.
[l]Reference 53.
[m]Reference 54.
[n]Reference 55.
[o]Reference 56.
[p]Reference 57.
[q]Reference 58.
[r]Reference 59.
[s]Reference 60.
[t]Reference 41.
[u]Reference 61.
[v]Reference 62.
[w]Reference 63.
[x]Reference 64.
[y]Reference 65.
[z]Reference 66.
[aa] Reference 67.

number of tin valence electrons. The aim of this section is to derive simple analytical expressions of N_s and N_p as functions of a small set of parameters describing the local environment of the tin atoms. These expressions are obtained from a molecular description of the tin chalcogenides for highly symmetrical Sn sites. For simplicity, the the tin chalcogenides of the present work will be denoted by $C_l\mathrm{Sn}_m X_P$, where *C* is the cation for the ternary compounds: $C=$Na, Ba, Ge, In, Sb, Tl, Pb, and Bi ($l=0$ for the binary compounds) and $X=$S, Se, and Te. Let us recall that the Sn and *C* atoms are surrounded by chalcogen nearest neighbors in all compounds.

The molecular model is obtained from the periodic method of Sec. III considering three main assumptions. The first approximation consists in neglecting the interactions between the *C* and *X* atoms. The periodic calculation of Sec. III gives positive charges for the *C* atoms in agreement with their cationic character. In order to evaluate the influence of

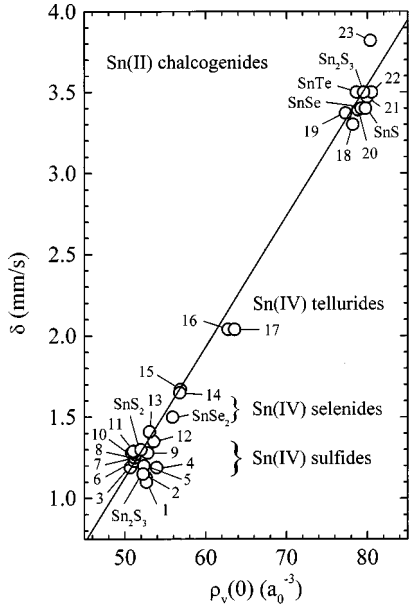

FIG. 3. Experimental values of the ^{119}Sn Mössbauer isomer shift δ against calculated values of the electron density at the nucleus $\rho_v(0)$ for tin chalcogenides. The numbering refers to the ternary chalcogenides given in Table II. The straight line is the linear correlation between δ and $\rho_v(0)$ obtained for binary tin compounds.

the C-X bonds on the tin electronic populations, calculations were also performed without the C-X bonds. For example, the C charges are equal to $+1$ for C=Na, In, and Tl, and $+3$ for C=Sb and Bi (perfect cations). This can be related to the atomic energy levels of the s, $E_s(C)$, and p, $E_p(C)$, valence electrons of the cations which are in the valence and conduction bands, respectively, except for Na and Ba which have only s valence electrons. In the latter case $E_s(C)$ is in the conduction band. The tin valence electron populations evaluated by the two approaches (with and without C-X bonds) only show small differences providing the same trends in the variations of $\rho_v(0)$. This means that the ternary compounds behave as a covalent tin-chalcogen network with a negative charge and isolated cations. The two other approximations allow one to transform the tin chalcogen network into simple molecular units. First, only the $5s(\mathrm{Sn})p(X)\sigma$ and $5p(\mathrm{Sn})p(X)\sigma$ two-center interactions are considered. Interactions with the chalcogen s valence orbitals are neglected because of their deep atomic energy levels compared to those of Sn.[20,21] Thus, the S $3s$, Se $4s$, and Te $5s$ states are assumed to be corelike states. The $pp\pi$ interactions between the p valence orbitals of Sn and X are not taken into account since they are smaller than the $pp\sigma$ interactions. The last approximation consists in a simplification of the local structure. In most of the materials considered in this work the chalcogen coordination number is lower or equal to 3, and the Sn-X-Sn bond angles are close to 90°. By considering the value of 90°, it is possible to form three orthogonal combinations of p-type valence orbitals for the chalcogens. Since there are only interactions between the Sn valence orbitals and combinations of p orbitals pointing toward the Sn atom, the tin-chalcogen network behaves as a set of noninteracting SnS_n units where the Sn coordination number n is fixed by the Sn local environment. In this work, only perfect tetrahedral ($n=4$) and octahedral ($n=6$) Sn environments are considered, since they concern most of the ternary chalcogenides and provide simple analytical expressions of the electronic populations.

B. Molecular electronic structures

By the model described in Sec. IV A, it can be shown that the molecular electronic structure of the $C_lSn_mX_p$ compounds is formed by the energy levels of the SnX_n molecules, the atomic energy levels of the s valence electrons of the chalcogen, $E_s(X)$, and those of the valence electrons of the cation, $E_s(C)$ and $E_p(C)$. In addition, for chalcogen coordination lower than 3 there is also a nonbonding state at $E_p(X)$. The orbital basis set of the SnX_n molecule is formed by the Sn $5s$ and Sn $5p$ orbitals, and by combinations of chalcogen p valence orbitals pointing toward the Sn atom. For tetrahedral and octahedral Sn environments the Hamiltonian matrix can be block diagonalized, leading to simple analytical expressions of the molecular energy levels and wave functions. For SnX_4 the diagonalization of the 8×8 Hamiltonian matrix gives a pair of bonding/antibonding s-like states (interactions between Sn $5s$ and S $3p$ orbitals) and a pair of bonding/antibonding threefold-degenerated p-like states (interactions between Sn $5p$ and S $3p$ orbitals). For SnX_6, the Hamiltonian is a 10×10 matrix, and the energy spectrum is formed by a pair of bonding/antibonding s-like states, a pair of bonding/antibonding threefold-degenerated p-like states, and a twofold-degenerated nonbonding p state at $E_p(X)$. For both the SnX_4 and SnX_6 molecules the bonding and antibonding molecular levels of the i-like states ($i=s,p$) can be written

$$E_{b,i}=E_p(X)+\beta_i[\gamma_i-(1+\gamma_i^2)^{1/2}], \tag{5}$$

$$E_{a,i}=E_p(X)+\beta_i[\gamma_i+(1+\gamma_i^2)^{1/2}], \tag{6}$$

where b and a denote the bonding and antibonding states, respectively, γ_i and β_i can be written in terms of the tight-binding parameters as

$$\gamma_i=\frac{E_i(Sn)-E_p(X)}{2\beta_i}, \tag{7}$$

$$\beta_s=\sqrt{6}sp\sigma \quad \text{for the } s\text{-like states of } SnX_6, \tag{8}$$

$$\beta_p=\sqrt{2}pp\sigma \quad \text{for the } p\text{-like states of } SnX_6, \tag{9}$$

$$\beta_s=\beta_p=\frac{sp\sigma+\sqrt{3}pp\sigma}{2} \quad \text{for } SnX_4. \tag{10}$$

As in Sec. III the atomic energies calculated by Herman and Skillman[20] and reported by Harrison[21] have been used for the intra-atomic parameters. For interactions between nearest neighbors, a d^{-2} scaling law,[21] where d is the interatomic distance, gives values of the two-center terms close to those obtained by the Robertson's rule used in Sec. III. Thus the $sp\sigma$ and $pp\sigma$ interactions have been related to the interatomic distance by this more simple d^{-2} scaling law. The main features of the electronic structures such as the positions of the peaks in the density of states may be qualitatively obtained from the analysis of the molecular levels. Such an approach is used here to characterize the oxidation states of tin. The following inequalities hold for all the chalcogenides considered in this work:

$$E_s(X)<E_{b,s}<E_{b,p}<E_p(X)<E_{a,s}<E_{a,p}. \quad (11)$$

The number of Sn $5s$ valence electrons is given by the occupancies of the two s-like states $E_{b,s}$ and $E_{a,s}$, and depends on the position of the Fermi level E_F obtained from the number of valence electrons in the unit cell. If E_F is greater than $E_{a,s}$, the two states $E_{b,s}$ and $E_{a,s}$ are occupied and $N_s(\mathrm{Sn})=2$. This corresponds to the Sn(II) oxidation state. If E_F is lower than $E_{a,s}$, the number of Sn $5s$ electrons is lower than 2 and is given by the occupancy of $E_{b,s}$. This corresponds to the Sn(IV) oxidation state. The number of Sn $5p$ electrons is given by the occupancy of the $E_{b,p}$ state, since $E_{a,p}$ is always greater than E_F. Let us consider for examples SnS_2, Tl_4SnS_4, and Tl_4SnTe_3. SnS_2 is formed by edge sharing SnS_6 octahedra, and the S atoms are bonded to three Sn atoms. Thus the molecular electronic structure is formed by the bonding and antibonding levels of the SnS_6 octahedron given by Eqs. (5)–(6), and the atomic levels $E_{3s}(S)$ and $E_{3p}(S)$. The highest occupied molecular level is obtained from the number of valence electrons (16 per unit cell) at $E_{3p}(S)$, in agreement with the expected Sn(IV) oxidation state. Since Tl_4SnS_4 may be viewed as consisting of isolated SnS_4 tetrahedra, the molecular electronic structure is formed by the bonding and antibonding states of these molecules and the atomic levels of the valence electrons of S and Tl. The Fermi level is also found at $E_{3p}(S)$ by considering the degeneracy of the levels and the number of valence electrons (40 per unit cell). Thus the Sn oxidation state is IV. By assuming for simplicity that Tl_4SnTe_3 is formed by isolated $SnTe_6$ octahedra, a molecular electronic structure similar to that of Tl_4SnS_4 is obtained: the same ordering of the molecular levels as given by Eq. (11), but not the same energy values. However, the degeneracy of the levels is modified due to the changes in the Sn site symmetry and in the number and the coordination of chalcogens. As a consequence the Fermi level is now found at $E_{a,s}$, and the Sn oxidation state is II. Thus this simple molecular picture allows to us distinguish the Sn(IV) and Sn(II) oxidation states of the two main families of tin chalcogenides observed by Mössbauer spectroscopy.

C. Tin electron populations

A more quantitative interpretation of the variations of δ for the Sn(IV) compounds requires the calculation of the numbers of Sn $5s$ and Sn $5p$ electrons. According to the molecular model the number of Sn valence electrons of type i $(i=s,p)$ is given by

$$N_i=2\sum_{l,E_l\leqslant E_F}|\langle\varphi_i|\psi_l\rangle|^2, \quad (12)$$

where E_l and ψ_l are the molecular energy levels and wave functions, respectively, of the SnX_n molecule, and φ_i is the tin atomic orbital of type i. As discussed above, the number of Sn $5s$ electrons is related to the occupancies of the $E_{b,s}$ and $E_{a,s}$ states. For Sn(II) compounds, these two levels are occupied and $N_s=2$, whereas the Sn(IV) compounds only the $E_{b,s}$ state is occupied. Since the $E_{a,p}$ state is always empty, the number of Sn $5p$ electrons for both the Sn(IV) and Sn(II) chalcogenides is given by the occupancy of the $E_{b,p}$ state. The numbers of Sn(IV) $5s$ and Sn $5p$ electrons can be written as

$$N_s=1-\alpha_s, \quad (13)$$

$$N_p=3(1-\alpha_p), \quad (14)$$

with

$$\alpha_i=\frac{\gamma_i}{\sqrt{1+\gamma_i^2}}, \quad (15)$$

where $i=s$, p, and γ_i is given by Eq. (7). The term α_i can be viewed as a polarity coefficient similar to that defined by Harrison for sp^3 compounds.[21]

Analytical expressions of N_s and N_p can be obtained from Eqs. (7)–(10) and (13)–(15) as a function of the intra-atomic energies $E_s(\mathrm{Sn})$, $E_p(\mathrm{Sn})$, and $E_p(X)$, the Sn site symmetry and the Sn-X average bond length. These expressions can be simplified because of the rather small variations of γ_s between about -0.8 and -0.3, and those of γ_p around 0.5, which allows a linearization of α_i defined by Eq. (15). Considering for simplicity SnS_4 as a reference molecule, the numbers of Sn valence electrons are written in terms of $\Delta E=E_p(X)$-$E_{3p}(\mathrm{S})$, where $E_{3p}(\mathrm{S})=-10.27$ eV and $\Delta d=d(\mathrm{Sn}$-$X)$-$d(\mathrm{Sn}$-$\mathrm{S})$ with $d(\mathrm{Sn}$-$\mathrm{S})=2.4$ Å. For SnX_4, this gives

$$N_s=1.305+0.230\,\Delta d+0.124\,\Delta E+0.103\;\Delta E\;\Delta d, \quad (16)$$

$$N_p=1.416-0.952\,\Delta d+0.264\,\Delta E+0.220\,\Delta E\;\Delta d, \quad (17)$$

and, for SnX_6,

$$N_s=1.236+0.185\,\Delta d+0.100\,\Delta E+0.083\,\Delta E\;\Delta d, \quad (18)$$

$$N_p=1.613-0.909\,\Delta d+0.252\Delta E+0.210\,\Delta E\;\Delta d. \quad (19)$$

Equations (16) and (18) show that the numbers of Sn $5s$ electrons for SnX_4 and SnX_6 increase with the atomic energy $E_p(X)$ and the distance $d(\mathrm{Sn}$-$X)$. This can be related to the decrease of the s-like bonding state $E_{b,s}$ relative to the Sn $5s$ state: $E_s(\mathrm{Sn})$-$E_{b,s}$ as the energy difference $E_p(X)$-$E_s(\mathrm{Sn})$ and/or the distance $d(\mathrm{Sn}$-$X)$ increase. The numbers of Sn $5p$ electrons given by Eqs. (17) and (19) increase with $E_p(X)$. Since $\Delta E_p<2$ eV, the second term (in Δd) on the right-hand side of Eqs. (17) and (19) is greater that the last term (in $\Delta E\;\Delta d$), and the decrease of Δd tends to increase N_p. The increase of N_p can be related to the increase of $E_{b,p}$ relative to the Sn $5p$ state: $E_p(\mathrm{Sn})$-$E_{b,p}$ due to the increase of $E_p(\mathrm{Sn})$-$E_p(X)$ and/or the decrease of $d(\mathrm{Sn}$-$X)$. Thus the increase of $E_p(X)$ tends to increase both N_s and N_p, whereas the increase of $d(\mathrm{Sn}$-$X)$ yields the increase of N_s and the decrease of N_p.

The electron density at the Sn nucleus is related to the numbers of Sn valence electrons by Eq. (3). However, a linear expression of $\rho_v(0)$ as a function of N_s and N_p gives for the Sn(IV) chalcogenides results which are close to those obtained by Eq. (3), and is therefore used here for simplicity. A linear interpolation of $\rho_v(0)$ to the values obtained for the Sn free ions by Ellis[19] gives

TABLE III. Typical data for Sn(IV) chalcogenides with tetrahedral SnX_4 and octahedral SnX_6 environments, where $X=$ S, Se, and Te, and for Sn(II) chalcogenides. The values of the Sn-X bond length d, the ^{119}Sn Mössbauer isomer shift relative to $BaSnO_3$, δ, the calculated numbers of tin valence electrons N_s(Sn) and N_p(Sn), and the calculated electron density at the nucleus $\rho_v(0)$ have been averaged over the different chalcogenide compounds given in Tables I and II.

	Sn(IV)S_4	Sn(IV)S_6	Sn(IV)Se_4	Sn(IV)Se_6	Sn(IV)Te_4	Sn(II)
d (Å)	2.4	2.6	2.55	2.7	2.8	
δ (mm/s)	1.3	1.2	1.7	1.5	2.0	3.2-3.8
N_s(Sn)	1.2	1.2	1.35	1.3	1.55	1.9-2
N_p(Sn)	1.4	1.4	1.5	1.5	1.6	0.9-1.5
$\rho_v(0)$ (a_0^{-3})	52	52	57	56	63	77-81

$$\rho_v(0)=6.6+39.6N_{5s}-3.7N_{5p}. \quad (20)$$

Putting expressions (16) and (17) into Eq. (20) gives, for SnX_4,

$$\rho_v(0)=53+12.6\ \Delta d+3.9\ \Delta E+3.3\ \Delta E\ \Delta d. \quad (21)$$

In the same way Eqs. (18)–(20) give, for SnX_6,

$$\rho_v(0)=49.6+10.7\,\Delta d+3\ \Delta E+2.5\,\Delta E\ \Delta d. \quad (22)$$

Equations (21) and (22) show that the electron density at the nucleus $\rho_v(0)$ increases with the Sn-X interatomic distance and the atomic energy level $E_p(X)$. This can be correlated to the increase of the number of Sn 5s electrons with ΔE and Δd. The values of N_s, N_p, and $\rho_v(0)$ have been evaluated considering the average distances reported in Table III. The values are given in Table IV, and are close to those obtained by the periodic tight-binding method (Table III). This validates the molecular calculation which therefore provides the correct trends in the variations of $\rho_v(0)$ as a function of the type of chalcogen and the Sn site symmetry. It is thus possible to relate the variations of the Mössbauer isomer shift to the Sn local environment from this model.

Experimentally, δ is found to increase for a given SnX_4 or SnX_6 environment for the sequence $X=$ S, Se, and Te. This result has been correlated to the increase of N_s and $\rho_v(0)$ obtained by both the periodic calculation (Table III) and the molecular model (Table IV). The energy of the chalcogen p valence electrons and the size of the anion both increase for the sequence S-Se-Te leading in the latter case to the increase of the Sn-X interatomic distance. As a consequence ΔE and Δd increase, which explains the increase of N_s and $\rho_v(0)$. Since the variations are lower than about 1.7 eV and 0.4 Å for ΔE and Δd, respectively, they both contribute to the variations of $\rho_v(0)$, and the observed increase of δ is due to the changes in both the type of chalcogen and the tin-chalcogen distance. As shown by Eqs. (17) and (19) the increase of N_p for the sequence S-Se-Te is due to the increase of ΔE, which is, however, partially canceled by that of Δd. This gives small variations for N_p which have a minor effect on $\rho_v(0)$.

Tables III and IV show that changes in the Sn site symmetry from SnX_4 to SnX_6 may be correlated to the decrease of δ and $\rho_v(0)$. From SnX_4 to SnX_6, the value of ΔE does not change, Δd increases by about 0.2 Å, and all the numerical coefficients of the right-hand side of Eqs. (21) and (22) decrease. The latter effect is more important than the increase of Δd, and explains the decrease of $\rho_v(0)$. As shown by comparison of Eqs. (16) and (18), this is also observed for N_s, which is the leading term in $\rho_v(0)$. It can be readily shown from Eqs. (8)–(10) that the decrease of the coefficients is mainly due to the decrease of the effective two-center interactions from SnX_6 to SnX_4. Although the Sn-X interactions $sp\sigma$ and $pp\sigma$ are stronger in SnX_4 than in SnX_6, the effective interaction β_i, which also depends on the number of chalcogens in the molecule, is greater for SnX_6 than for SnX_4. Thus the observed decrease of δ from tetrahedral to octahedral Sn environments may be roughly related to the increase of the number of chalcogen nearest neighbors.

V. CONCLUSIONS

The observed main trends in the variations of the ^{119}Sn Mössbauer isomer shift δ for tin chalcogenides have been explained from a tight-binding calculation of the electron density at the nucleus. The interpretation has been carried out along the following three steps. First the values of $\rho_v(0)$ have been evaluated by a tight-binding calculation for a large number of tin binary compounds. The variations of $\rho_v(0)$ have been favorably compared to previously published results, which may be considered as a good test of the accuracy of the present approach. Second, the values of $\rho_v(0)$ have been evaluated for ternary tin chalcogenides and have been correlated to the variations of the experimental values of δ. Different families of tin chalcogenides have been distin-

TABLE IV. Values of the numbers of tin valence electrons N_s(Sn) and N_p(Sn) and of the electron density at the nucleus $\rho_v(0)$ obtained from the molecular calculation.

	SnS_4	SnS_6	$SnSe_4$	$SnSe_6$	$SnTe_4$
N_s(Sn)	1.30	1.27	1.44	1.38	1.67
N_p(Sn)	1.42	1.43	1.49	1.57	1.63
$\rho_v(0)$ (a_0^{-3})	53.0	51.7	58.1	55.6	66.8

guished considering the Sn oxidation state, the Sn site symmetry, and the type of chalcogen. The observed main trends in the variations of δ have been explained from changes in the calculated number of tin valence electrons. Finally, a molecular model has been proposed in order to relate the changes in the electronic populations to the Sn local environments. For Sn(IV) chalcogenides, analytical expressions of $\rho_v(0)$ have been derived as a function of the Sn site symmetry, the type of chalcogen and the tin-chalcogen bond length providing a simple explanation of the experimental variations of δ.

ACKNOWLEDGMENTS

The author wishes to thank Dr. J. Olivier-Fourcade and Dr. J. C. Jumas for many useful discussions. The research was performed under a European Research Network Program (PICS Grant No. 505) initiated by the Centre National de la Recherche Scientifique (France). Computer resources provided by the Centre National Universitaire Sud de Calcul (France) under Project No. C98092 are gratefully acknowledged.

*Electronic address: lippens@univ-montp2.fr

[1] N. N. Greenwood and T. C. Gibb, *Mössbauer Spectroscopy* (Chapman and Hall, London, 1971).
[2] *Mössbauer Isomer Shifts*, edited by G. K. Shenoy and F. E. Wagner (North-Holland, Amsterdam, 1978).
[3] *Mössbauer Spectroscopy Applied to Inorganic Chemistry*, edited by G. J. Long (Plenum, New York, 1984).
[4] *Electron and Phonons in Layered Crystal Structures*, edited by T. J. Wieting and M. Schlüter (Reidel, Dordrecht, 1979).
[5] R. H. Williams, R. B. Murray, D. W. Govan, J. M. Thomas, and E. L. Evans, J. Phys. C **6**, 3631 (1973); R. B. Murray and R. H. Williams, *ibid.* **6**, 3643 (1973).
[6] R. B. Shalvoy, G. B. Fisher, and P. J. Stiles, Phys. Rev. B **15**, 2021 (1977).
[7] A. Svane and E. Antocik, Phys. Rev. B **35**, 4611 (1987).
[8] A. Svane, N. E. Christensen, C. O. Rodriguez, and M. Methfessel, Phys. Rev. B **55**, 12 572 (1997).
[9] M. Grodzicki, V. Männing, A. X. Trautwein, and J. M. Friedt, J. Phys. B **20**, 5595 (1987).
[10] J. Terra and D. Guenzburger, Phys. Rev. B **39**, 50 (1989).
[11] J. Terra and D. Guenzburger, J. Phys.: Condens. Matter **3**, 6763 (1991).
[12] J. C. Slater and G. F. Koster, Phys. Rev. **94**, 1494 (1954).
[13] J. Robertson, J. Phys. C **12**, 4753 (1979).
[14] J. Robertson, Phys. Rev. B **28**, 4671 (1983).
[15] P. E. Lippens, J. Olivier-Fourcade, J. C. Jumas, S. Dupont, A. Gheorghiu, and C. Sénémaud, Phys. Rev. B **56**, 13 054 (1997).
[16] P. E. Lippens and L. Aldon, Solid State Commun. **108**, 913 (1998).
[17] B. P. Dunlap and G. M. Kalvius, in *Mössbauer Isomer Shifts* (Ref. 2), Chap. 2.
[18] G. K. Shenoy and B. D. Dunlap, in *Mössbauer Isomer Shifts* (Ref. 2), Appendix IV.
[19] S. L. Ruby and G. K. Shenoy, in *Mössbauer Isomer Shifts* (Ref. 2), Chap. 9b.
[20] F. Herman and S. Skillman, *Atomic Structure Calculations* (Prentice-Hall, Englewood Cliffs, NJ, 1963).
[21] W. A. Harrison, in *Electronic Structure and Properties of Solids* (Freeman, San Francisco, 1980).
[22] W. A. Harrison, Phys. Rev. B **24**, 5835 (1981).
[23] J. G. Stevens and M. A. Goforth, *^{119}Sn Mössbauer Spectroscopy* (Mössbauer Effect Data Center, Asheville, NC, 1993).
[24] R. Hoppe and W. Dähne, Naturwissenschaften **49**, 254 (1962).
[25] N. Ruchaud, C. Mirambet, L. Fournes, J. Grannec, and J. L. Soubeyroux, Z. Anorg. Allg. Chem. **590**, 173 (1990).
[26] M. F. A. Dove, R. King, and J. King, J. Chem. Soc. Chem. Commun. **24**, 944 (1973); R. King, Ph.D. thesis, University of Nottingham, 1974.
[27] W. H. Baur, Acta Crystallogr. **9**, 515 (1956).
[28] P. von Brand and H. Sackmann, Acta Crystallogr. **16**, 446 (1963).
[29] R. Kniep, D. Mootz, U. Severin, and H. Wunderlich, Acta Crystallogr., Sect. B: Struct. Crystallogr. Cryst. Chem. **38**, 2022 (1982).
[30] R. W. G. Wyckoff, *Crystal Structures* (Wiley, New York, 1964).
[31] F. Meller and I. Fankuchen, Acta Crystallogr. **8**, 343 (1955).
[32] P. C. Donohue, Inorg. Chem. **9**, 335 (1970).
[33] P. Eckerlin and W. Kischio, Z. Anorg. Chem. **363**, 1 (1968).
[34] F. Izumi, J. Solid State Chem. **38**, 381 (1981).
[35] H. Wiedemeir and H. G. von Schnering, Z. Kristallogr. **148**, 295 (1978).
[36] G. Will and M. O. Bargouth, Z. Kristallogr. **153**, 89 (1980).
[37] R. A. Howie, W. Moser, and I. C. Trevena, Acta Crystallogr., Sect. B: Struct. Crystallogr. Cryst. Chem. **28**, 2965 (1972).
[38] J. M. van den Berg, Acta Crystallogr. **14**, 1002 (1961).
[39] J. Grannec, L. Fournès, P. Lagassié, P. Hagenmuller, and J. C. Cousseins, Mater. Res. Bull. **25**, 815 (1990).
[40] L. Fournès, J. Grannec, Y. Potin, and P. Hagenmuller, Solid State Commun. **59**, 833 (1986).
[41] J. C. Jumas, J. Olivier-Fourcade, M. Ribes, E. Philippot, and M. Maurin, Bull. Soc. Chim. Fr. **11**, 37 (1980).
[42] C. Adenis, J. Olivier-Fourcade, J. C. Jumas, and E. Philippot, Rev. Chim. Miner. **23**, 735 (1986).
[43] J. C. Jumas, J. Olivier-Fourcade, E. Philippot, and M. Maurin, Rev. Chim. Miner. **16**, 48 (1979).
[44] J. C. Jumas, M. Ribes, E. Philippot, and M. Maurin, C. R. Seances Acad. Sci., Ser. C **275**, 269 (1972).
[45] K. Susa and H. Steinfink, J. Solid State Chem. **3**, 75 (1971).
[46] Y. Piffard, M. Tournoux, A. L. Ajavon, and R. Eholié, Rev. Chim. Miner. **21**, 56 (1984).
[47] J. C. Jumas, F. Vermot-Gaud-Daniel, and E. Philippot, Cryst. Struct. Commun. **2**, 157 (1973).
[48] J. C. Jumas, E. Philippot, and M. Maurin, J. Solid State Chem. **14**, 152 (1975).
[49] J. C. Jumas, E. Philippot, F. Vermot-Gaud-Daniel, M. Ribes, and M. Maurin, J. Solid State Chem. **14**, 319 (1975).
[50] G. Eulenberger, Z. Naturforsch. B **36**, 687 (1981).
[51] J. C. Jumas, J. Olivier-Fourcade, F. Vermot-Gaud-Daniel, M. Ribes, E. Philippot, and M. Maurin, Rev. Chim. Miner. **11**, 13 (1974).
[52] Y. Piffard, M. Tournoux, A. L. Ajavon, and R. Eholié, Rev. Chim. Miner. **21**, 21 (1984).
[53] K. O. Klepp, Monatsch. Chem. **115**, 1133 (1984).
[54] S. Jaulmes and P. Houenou, Mater. Res. Bull. **15**, 911 (1980).
[55] G. Akinocho, P. Houenou, S. Oyetola, R. Eholie, J. C. Jumas, J. Olivier-Fourcade, and M. Maurin, J. Solid State Chem. **93**, 336 (1991).

[56] V. Agafonov, B. Legendre, N. Rodier, J. M. Cense, E. Dichi, and G. Kra, Acta Crystallogr., Sect. C: Cryst. Struct. Commun. **47**, 850 (1991).
[57] V. Agafonov, B. Legendre, N. Rodier, J. M. Cense, E. Dichi, and G. Kra, Acta Crystallogr., Sect. C: Cryst. Struct. Commun. **47**, 1300 (1991).
[58] T. B. Zhukova and A. I. Zaslavskii, Kristallografiya **16**, 918 (1971) [Sov. Phys. Crystallogr. **16**, 796 (1972)].
[59] S. Bradtmöller and P. Böttcher, Z. Anorg. Allg. Chem. **619**, 1155 (1993).
[60] J. Fenner and D. Mootz, Z. Anorg. Allg. Chem. **427**, 128 (1976).
[61] R. Greatrex, N. N. Greenwood, and M. Ribes, J. Chem. Soc. Dalton Trans. **6**, 500 (1976).
[62] A. Ibanez, J. C. Jumas, E. Philippot, A. L. Ajavon, and R. Eholié, Rev. Chim. Miner. **23**, 281 (1986).
[63] G. Akinocho, P. Houenou, S. Oyetola, R. Eholié, J. Olivier-Fourcade, J. C. Jumas, and M. Maurin, J. Soc. Quest Afr. Chi. **1**, 10 (1996).
[64] E. Dichi, G. Kra, R. Eholié, G. Zégbé, M. L. Elidrissi Moubtassim, J. C. Jumas, J. Olivier-Fourcade, and G. Langouche, J. Solid State Chem. **112**, 31 (1994).
[65] F. Ledda, C. Muntoni, S. Serci, and L. Pellerito, Chem. Phys. Lett. **134**, 545 (1987).
[66] G. Concas, T. M. de Pascale, L. Garbato, F. Ledda, F. Meloni, A. Rucci, and M. Serra, J. Phys.: Chem. Solids **53**, 791 (1992).
[67] A. von Feltz, E. Schlenzig, and D. Arnold, Z. Anorg. Allg. Chem. **403**, 243 (1974).